

Instance-Aware Generalized Referring Expression Segmentation

E-Ro Nguyen¹ Hieu Le² Dimitris Samaras¹ Michael Ryoo¹
¹Stony Brook University ²EPFL

Abstract

Recent works on Generalized Referring Expression Segmentation (GRES) struggle with handling complex expressions referring to multiple distinct objects. This is because these methods typically employ an end-to-end foreground-background segmentation and lack a mechanism to explicitly differentiate and associate different object instances to the text query. To this end, we propose InstAlign, a method that incorporates object-level reasoning into the segmentation process. Our model leverages both text and image inputs to extract a set of object-level tokens that capture both the semantic information in the input prompt and the objects within the image. By modeling the text-object alignment via instance-level supervision, each token uniquely represents an object segment in the image, while also aligning with relevant semantic information from the text. Extensive experiments on the gRefCOCO and Ref-ZOM benchmarks demonstrate that our method significantly advances state-of-the-art performance, setting a new standard for precise and flexible GRES.

1. Introduction

Referring Expression Segmentation (RES) aims to segment the objects described by an input language expression. Standard RES approaches [6, 8, 26, 34] mainly focus on single-target scenarios with the input expression describing a single object, e.g., “the kid in red”. Generalized Referring Expression Segmentation (GRES) broadens this scope to handle more complex cases, including expressions that refer to multiple objects, such as “all people,” or cases where the input image may not contain any valid target.

To handle GRES, recent works [7, 17, 25, 29] utilize transformer-based architectures to improve the multimodal interaction. ReLA [17] models the complex interactions among regions and the dependencies between different parts of the image and words in the expression. LQMFormer [29] addresses query collapse and performs query selection through a multi-modal query feature fusion technique. HDC [25] enhances the decoding process through a hierarchical scheme with object counting to model complete semantic context. Despite these ad-

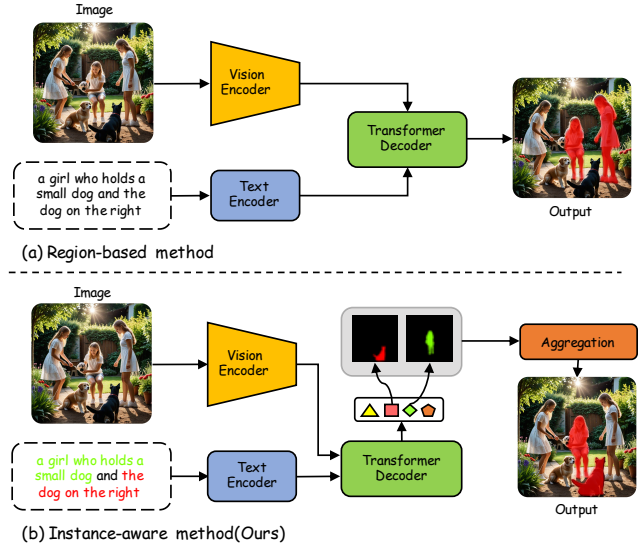


Figure 1. (a) Previous GRES methods typically output a single foreground mask in an end-to-end manner, struggling with complex cases involving multiple referred object instances. In contrast, our proposed method automatically localizes relevant object instances associated with different parts of the input prompt before aggregating them to produce the final mask (b).

vances, all these methods share a common limitation: they all follow an end-to-end approach that predicts a single foreground-background mask and lack an explicit mechanism to differentiate and associate individual object instances with specific parts of the text query. Consequently, they struggle with complex prompts referring to multiple distinct objects, leaving such cases as an open challenge. For example, when asked to segment “the girl who holds a small dog and the dog on the right” in the image shown in Fig. 1, most methods either segment all girls and dogs indiscriminately or get inaccurate segments, as observed with the state-of-the-art GRES method ReLA [17]. Thus, we need a model to explicitly predict and link relevant objects to specific semantic entities of the input text, to accurately segment each object described in complex expressions.

To this end, we introduce InstAlign, a novel GRES model that incorporates instance-level reasoning into the segmentation process. Our approach is simple but effective; we adapt the instance segmentation framework [3, 4, 14] to

identify and segment only object instances described in the prompt. To facilitate this, we design a novel loss function to constrain each segmented object to explicitly link to specific semantic entities of the input text. Thus, InstAlign learns to parse both the input text and images into small components to establish explicit connections between the input expression and the corresponding objects in the image.

Specifically, we integrate text prompt inputs in a query-based instance segmentation architecture, Mask2Former [4], and guide this model to identify and segment only object instances in the image that correspond to the input expression. To achieve this, we ensure that each segmented object is precisely linked to the specific semantic component (*i.e.*, phrase) of the input text describing it. We enforce this through our proposed Phrase-Object Alignment loss function, which explicitly identifies the text phrase from the input expression that best corresponds to each segmented object and strengthens this association. This alignment ensures that the model not only identifies and segments the correct objects but also captures the fine-grained relationships between textual phrases and visual instances.

Further, we propose two modules to adapt the instance segmentation framework to the GRES setting: an Adaptive-Instance-Aggregation (AIA) module and a no-target prediction head. AIA automatically integrates all segmented object instances based on their relevance scores to predict the final mask. This enhances the model’s focus on the most relevant instances, thereby improving segmentation performance and robustness in complex GRES scenarios. The no-target prediction head aggregates both text and object instance features to accurately predict the target-absent cases.

We evaluate InstAlign on two widely used benchmarks for GRES: gRefCOCO [17] and Ref-ZOM [7]. Our experiments demonstrate that InstAlign significantly outperforms state-of-the-art GRES methods and LLM-based approaches [2, 13, 37]. The results highlight InstAlign’s ability to handle complex referring expressions, setting a new standard in the field. Our main contributions are:

- We propose InstAlign, the first instance-aware approach to GRES that effectively handles complex multi-object scenarios by explicitly differentiating and associating individual object instances with specific phrases in the text.
- We introduce a phrase-object alignment mechanism, enabling our model to link each segmented object with the corresponding semantic part of the input text.
- We develop an Adaptive Instance Aggregation module that dynamically integrates segmented object instances based on their relevance scores, improving overall segmentation performance.
- Our method achieves state-of-the-art performance on standard GRES benchmarks, significantly improving segmentation accuracy. On gRefCOCO, InstAlign achieves a gIoU of 74.34% and N-acc of 79.72%, outperforming previous methods by 3.3% and 12.25%, respectively.

2. Related Work

The vision community has widely adopted Transformer-based architectures [5, 9, 11, 18, 19, 30, 31, 33, 36, 38, 40] to solve RES task. VLT [6] uses cross-attention to produce vector queries from multimodal features. Similarly, LAVT [40] shows that early cross-modal fusion of features improves alignment. CRIS [34] leverages CLIP’s robust image-text alignment capabilities to perform pixel-text contrastive learning. VATEX [27] decomposes language cues into object and context understanding and leverages vision-aware text features to improve text understanding. Recently, ReMamber [39] integrates the power of Mamba to explicitly model image-text interaction while Mask Grounding [5] explicitly learns the correspondence between text and visual tokens.

ReLA [17] introduces a region-based GRES baseline that models the relationship both among different image regions and between regions and words. DMMI [7] introduces two decoder branches for bidirectional information flow, where the text-to-image decoder localizes the target based on text queries, and the image-to-text decoder reconstructs erased entity phrases to enhance visual feature representations. LMQFormer [29] enhances segmentation with Gaussian-based fusion, dynamic query focus, and an auxiliary loss to prevent query collapse.

Mask2Former [4] pioneered instance segmentation by leveraging a Transformer-based architecture, applying Hungarian matching [1, 12] between predicted instances and ground truth based on both class and mask costs. Building on this, ReferFormer [35] and VATEX [27] integrate instance matching in the context of referring expressions, focusing on segmenting a single object per expression. Both models utilize instance-matching mechanisms to align object query and target object described in the language input, getting precise segmentation in one-to-one scenarios. However, their reliance on binary segmentation limits their performance when handling expressions involving multiple objects or ambiguous descriptions, as they lack the capacity for multi-instance differentiation.

3. Method

3.1. Overview

Figure 2 summarizes our proposed method, InstAlign, which leverages both visual and textual inputs to generate instance-aware segmentation masks. InstAlign utilizes a transformer-based architecture that processes object queries (*i.e.*, tokens) to generate multiple instance masks via an instance-aware segmentation framework [4]. We integrate text prompt inputs into this model and guide it to only segment instance masks of objects specified in the input prompt. To achieve this, we begin with a set of N randomly initialized object queries and progressively refine them, utilizing both image and text features to correctly associate

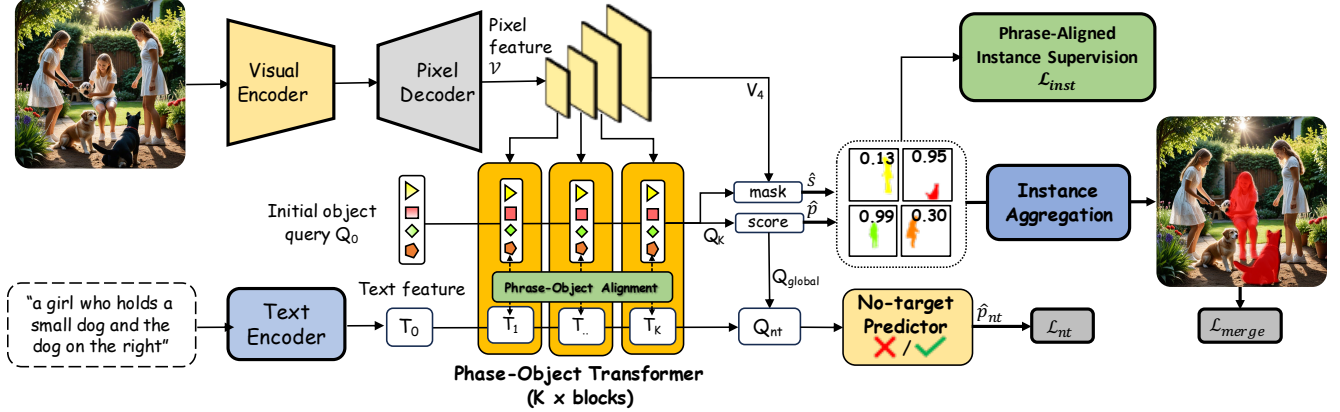


Figure 2. **Overview of InstAlign.** Our proposed method identifies object queries that produce only instance masks of objects specified in the input prompt. To achieve this, we begin with a set of initial object queries and progressively refine them, utilizing both image and text features to associate each query with a targeted object instance in the image as well as a phrase extracted from the input text.

each query with a targeted object instance in the image as well as a phrase extracted from the input text.

This progressive refinement is conducted via K Phrase-Object Transformer blocks that we introduce, which takes the multi-scale visual features \mathcal{V} , text features T_0 , and object queries $Q_0 \in \mathbb{R}^{N \times C}$ as input, to output a refined text feature T_K and object queries Q_K (Sec. 3.3). The resulting object queries are used to obtain a set of instance segment masks, each associated with a relevance score. The model is trained to identify and segment only objects relevant to the input prompt via instance supervision (Sec. 3.4). This process is facilitated via our proposed Phrase-Object Alignment loss (Sec. 3.3.1), which enforces each object query to be precisely linked to the specific semantic component of the input text describing it. It is important to note that, similar to prior works [3, 4], the number of object queries N does not need to equal the actual number of relevant objects. The instance supervision enables the model to refine only object queries that correspond to relevant instances and enforce unmatched queries to be irrelevant to the input prompt throughout the whole refinement process.

The resulting instance predictions are then adaptively combined in the Instance Aggregation module, which weighs each instance based on its relevance score, allowing for precise segmentation without fixed selection (Sec. 3.5). Finally, a No-Target Predictor uses both the final object queries Q_K and the enhanced text features T_K to determine if the expression points to any target in the image (Sec. 3.6). If "no-target" is predicted during inference, the final output is an all-zero segmentation mask.

3.2. Feature Extraction

To extract the text information, we adopted RoBERTa [21] to embed the input expression into high-level word features $T_0 \in \mathbb{R}^{L \times C}$, where C and L denotes the number of channels and the length of the expression, respectively. We use an encoder-decoder architecture to extract the multi-scale

pixel features $\mathcal{V} = \{V_i \in \mathbb{R}^{C \times H_i \times W_i}\}_{i=1}^4$ from the input image. Here, H_i and W_i denote the height and the width of the feature maps in the i -th stage, respectively. As in [4], these visual features V_i are obtained from the Pixel Decoder [4, 43].

3.3. Phrase-Object Transformer

Given a set of randomly initialized object queries along with the extracted text and visual features, we apply multiple blocks of our Phrase-Object Transformer, illustrated in Fig. 3. These blocks' purpose is to iteratively integrate visual and textual features into the object queries while simultaneously embedding the information from the object queries into the text features. This bidirectional feature aggregation, guided by our Phrase-Object Alignment loss, enables associating each relevant object instance in the image to an object query and the corresponding text phrase features.

More specifically, the k -th transformer block takes as input the pixel features $V_k \in \mathbb{R}^{H_k \times W_k \times C}$, text features $T_{k-1} \in \mathbb{R}^{L \times C}$, and object query $Q_{k-1} \in \mathbb{R}^{N \times C}$ and outputs refined object query Q_k and text features T_k . Similar to Mask2Former [4], visual features at specific scales are input to different blocks in a round-robin manner and where V_k denotes the visual features input to the k -th transformer block. We employ an Object-Text Cross Attention layer with a bidirectional attention mechanism [5, 7, 27, 38], allowing both text features and object queries to be transformed based on information from both sides. To obtain the refined object queries Q_k , we pass the object queries Q_{k-1} sequentially through a cross-attention layer with visual features V_k , an Object-Text Cross Attention layer with text features T_{k-1} , a self-attention layer, and an FFN layer. Simultaneously, the text features T_{k-1} are passed through the same Object-Text Cross Attention layer to produce the refined text features T_k .

Previous approaches [5, 7, 27, 38] usually directly enhance the text features by using pixel features. In contrast,

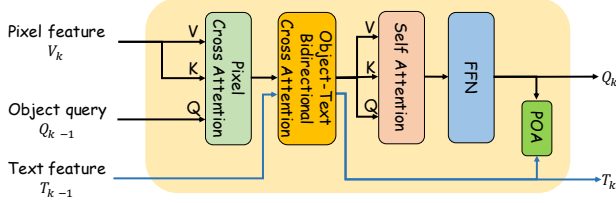


Figure 3. **Phrase-Object Transformer.** We employ an Object-Text Cross Attention layer with a bidirectional attention mechanism allowing both text features and object queries to be transformed based on information from both sides.

we enhance them by using object queries. This mechanism not only produces a much smaller memory footprint as it avoids computing attention weights with high-resolution pixel feature maps, but it can also produce mutual interaction at the object level instead of the pixel-wise level.

3.3.1. Phrase-Object Alignment Loss

Our proposed Phrase-Object Alignment (POA) loss, illustrated in Fig. 4 improves the alignment between object features and the semantics of the text expression, ensuring that each object query aligns closely with the relevant part of the input text. This step enhances the model’s ability to associate specific object instances with language cues, particularly in complex scenarios involving multiple instances.

We first derive the phrase-object relevant scores R_k from the affinity between the text features T_k and the object queries Q_k . These scores quantify the alignment of each object feature with the text features, effectively weighting the text features by their relevance to the objects. The phrase features $P_k \in \mathbb{R}^{N \times C}$ of N objects are then obtained by the weighted sum of text features using the relevance scores:

$$R_k = \text{softmax}\left(\frac{Q_k T_k^\top}{\sqrt{C}}\right) \quad (1)$$

$$P_k = R_k T_k \quad (2)$$

Then, the alignment loss $\mathcal{L}_{phrase}(i)$ for the i -th object is then calculated based on the similarity between the obtained phrase feature P_k^i of this object and the object query Q_k^i :

$$\mathcal{L}_{phrase}(i) = 1 - \text{sim}(P_k^i, Q_k^i), \quad (3)$$

where sim denotes the cosine similarity. This loss quantifies how well each object query aligns with the semantic part of the prompt that best describes it. Minimizing this loss, therefore, encourages the model to modify the text features and object queries to strengthen their alignment. This is demonstrated in Fig. 6, where it visualizes one object query, its corresponding segment, and its relevant text phrase parsed from the input text (highlighted in red). In the next section, we describe how we incorporate this alignment loss into our instance segmentation framework.

3.4. Phrase-Aligned Instance Supervision

After refining the object queries through the Phrase-Object Transformer (POT), our next goal is to produce accurate

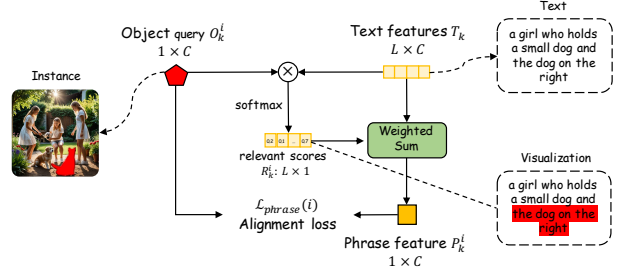


Figure 4. **Phrase-Object Alignment Loss.** Given an object query, we first compute a text feature embedding representing a text phrase that best aligns with the query (highlighted in red). Then, our phrase-object alignment loss penalizes the cosine difference between the object query and this phrase feature.

object instance masks of only objects relevant to the input prompt from these object queries. We supervise this system via instance-aware segmentation losses [3, 4] that encourage object queries to output targeted masks, and our proposed POA loss function that strength the association of each object query to a particular textual phrase parsed from the input prompt. This approach ensures that our model not only segments relevant instances individually but also aligns them semantically with the input expression.

Prediction Heads. Given a refined object query $Q_K \in \mathbb{R}^{N \times C}$, we first predict the probability $\hat{p} \in \mathbb{R}^N$ of these instances being related to the expression input via a score prediction head. Similar, N instance masks $\hat{s} \in \mathbb{R}^{\frac{H}{4} \times \frac{W}{4} \times N}$ associated to this object query can be computed by:

$$\hat{s} = V_4 \cdot Q_K^\top, \quad (4)$$

where $V_4 \in \mathbb{R}^{\frac{H}{4} \times \frac{W}{4} \times C}$ is the pixel features at the high-resolution scale extracted from the Pixel Decoder (Sec. 3.2)

Instance Matching and Objective Functions. The ground truth segmentation $\mathcal{M}_{gt} \in \mathbb{R}^{H \times W}$ is constructed by combining a set of M ground-truth instance segments $s = \{s_i\}_{i=1}^M$. To supervise our predictions effectively, we must first establish a one-to-one correspondence between the predicted instances and the ground-truth instances. We achieve this by utilize Hungarian Matching [4, 12] to find the optimal set of prediction indices $\omega^* = \{\omega_i\}_{i=1}^M$ that minimizes the following matching cost:

$$\omega^* = \arg \min_{\omega \subseteq [N]} \sum_{i=1}^M \mathcal{L}_{\text{match}}(\omega_i, i), \quad (5)$$

where the per-instance matching cost $\mathcal{L}_{\text{match}}$ for i -th predicted instance and j -th ground-truth instance is defined as:

$$\mathcal{L}_{\text{match}}(i, j) = \lambda_{\text{score}} \mathcal{L}_{\text{score}}(\hat{p}_i, 1) + \lambda_{\text{mask}} \mathcal{L}_{\text{mask}}(\hat{s}_i, s_j) + \lambda_{\text{phrase}} \mathcal{L}_{\text{phrase}}(i) \quad (6)$$

Here, $\mathcal{L}_{\text{score}}$ is the BCE loss that promotes high confidence for relevant instances, $\mathcal{L}_{\text{mask}}$ is the combination of dice loss [32] and BCE loss, and $\mathcal{L}_{\text{phrase}}$ enhances the alignment

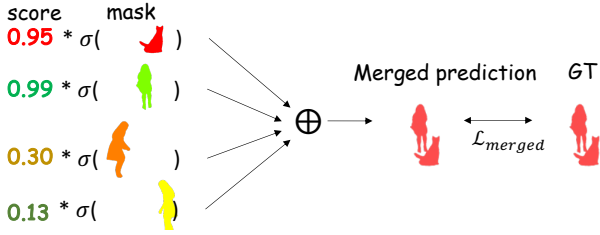


Figure 5. **Adaptive Instance Aggregation.** We use σ for the PReLU activation.

between the object query with the corresponding expression phrase. The hyper-parameters λ_{score} , λ_{mask} , λ_{phrase} control the balance of each component in the matching cost.

After determining the optimal match, we define the instance loss \mathcal{L}_{inst} to optimize the model for both matched and unmatched samples. The total instance loss is given by:

$$\mathcal{L}_{inst} = \sum_{i=1}^M \mathcal{L}_{match}(\omega_i^*, i) + \sum_{i=1, i \notin \omega^*}^N \mathcal{L}_{score}(\hat{p}_i, 0), \quad (7)$$

where the first term ensures that for each matched instance, the model minimizes the combined matching loss while the second term penalizes unmatched instances by encouraging their relevance scores \hat{p}_i to approach zero, indicating irrelevance to the expression.

3.5. Instance Aggregation

The goal of GRES is to generate a single binary segmentation map of relevant pixels. Given N candidate instances and their corresponding relevant scores, $\{\hat{s}_i, \hat{p}_i\}_{i=1}^N$, we aim to properly select and aggregate only instances that correspond to the referring expression. A straightforward method is to only select instances with relevance scores exceeding a fixed threshold [42]. However, this method may yield inconsistent results by either including irrelevant instances or excluding relevant ones that fail to surpass the threshold. Instead, we propose an Adaptive Instance Aggregation (AIA) module as illustrated in Figure 5.

This module dynamically adjusts the weighting of instances based on their relevance scores. This allows instances with higher scores to contribute more significantly to the final segmentation, while lower-scored instances are down-weighted, providing a more flexible mechanism for identifying and merging relevant object segments. Additionally, we apply a PReLU activation to the segmentation masks before merging, effectively suppressing negative values associated with irrelevant or background regions.

The final merged segmentation mask is computed as:

$$\mathcal{M}_{merged} = \text{Sigmoid}\left(\sum_{i=1}^N (\hat{p}_i \cdot \text{PReLU}(\hat{s}_i))\right) \quad (8)$$

We supervise the merging process, via a mask loss between the final merged mask \mathcal{M}_{merged} and ground-truth mask \mathcal{M}_{gt} .

$$\mathcal{L}_{merged} = \mathcal{L}_{mask}(\mathcal{M}_{merged}, \mathcal{M}_{gt}) \quad (9)$$

This loss encourages the final merged mask to closely match the ground truth, effectively guiding both the instance predictions and the adaptive aggregation. In essence, simply selecting masks with scores exceeding a threshold is analogous to a hard-assignment method, while our weighting function represents a soft-assignment approach, providing greater flexibility and robustness in segment merging. We verify its effectiveness in the ablation study (Section 4.3)

3.6. No-target Predictor

No-target is a challenging GRES scenario where the input expression does not refer to any object in the image. Some prior methods formulate this by directly forcing the segmentation prediction into an all-zero case [7, 34, 40] or using object counting [25] to improve no-target prediction. Recent works like ReLA [17] and LQMFormer [29] predict the no-target likelihood by averaging all object queries. However, averaging all queries equally can lead to inaccuracies, especially when small target objects are overlooked due to dominant non-target regions.

To address this, we propose a method that leverages both object queries and text features and prioritizes object queries based on their relevance scores. Specifically, we compute a weighted sum of instance representations to form a global token $Q_{global} \in \mathbb{R}^C$.

$$Q_{global} = \sum_{i=1}^N (\hat{p}_i \cdot Q_K^i), \quad (10)$$

where Q_K^i is the i -th refined object query and \hat{p}_i is its relevance score. We also extract a sentence-level text feature $T_{sen} \in \mathbb{R}^C$ by averaging word-level features T_K : $T_{sen} = \text{Average}(T_K, \text{dim} = 0)$.

Combining Q_{global} and T_{sen} into a unified representation Q_{nt} provides a comprehensive view that captures both instance and sentence-level context, allowing us to accurately predict the no-target likelihood \hat{p}_{nt} :

$$Q_{nt} = \text{Concat}(Q_{global}, T_{sen}) \quad (11)$$

$$\hat{p}_{nt} = \text{MLP}(Q_{nt}) \quad (12)$$

3.7. Training Objectives

We supervise our framework with three training objectives:

- 1) Final mask supervision \mathcal{L}_{merged} which is the combination of dice loss [32] and BCE loss; 2) $\mathcal{L}_{instance}$, which guides the association between object queries, targeted object masks, and relevant input text phrases (section 3.4); and 3) \mathcal{L}_{nt} , which is a BCE loss measuring the existence of instances [17]. Therefore, the total loss can be formulated as:

$$\mathcal{L}_{total} = \lambda_{merged} \mathcal{L}_{merged} + \lambda_{inst} \mathcal{L}_{inst} + \lambda_{nt} \mathcal{L}_{nt}, \quad (13)$$

where λ_{merged} , λ_{inst} , λ_{nt} are the scalar coefficients.

Method	Backbone	val			testA			testB		
		cIoU	gIoU	N-acc	cIoU	gIoU	N-acc	cIoU	gIoU	N-acc
<i>LLM-based Methods</i>										
LISA-7B [†] [13]	SAM-ViT-H	61.63	61.76	54.67	68.5	66.27	50.01	60.63	58.84	51.91
GSVA-7B [†] [37]	SAM-ViT-H	63.29	66.47	62.43	69.93	71.08	65.31	60.47	62.23	60.56
SAM4MLLM-7B [†] [2]	SAM-EffViT-XL1	65.66	68.37	63.71	69.62	69.05	65.96	62.35	63.71	61.25
<i>RES Methods</i>										
MattNet [42]	ResNet-101	47.51	48.24	41.15	58.66	59.30	44.04	45.33	46.14	41.32
VLT [6]	DarkNet-53	52.61	52.00	47.17	62.19	63.20	48.74	50.52	50.88	48.46
CRIS [34]	ResNet-101	55.34	56.27	-	63.82	63.42	-	51.04	51.79	-
LAVT [40]	Swin-B	57.64	58.40	49.32	65.32	65.90	49.25	55.04	55.83	48.46
<i>GRES Methods</i>										
ReLA [17]	Swin-B	62.42	63.60	56.37	69.26	70.03	59.02	59.88	61.02	58.40
LQMFormer [29]	Swin-B	64.98	70.94	67.47	-	-	-	-	-	-
MABP [15]	Swin-B	65.72	68.86	62.18	71.59	72.81	-	62.76	64.04	-
HDC [25]	Swin-B	65.42	68.23	63.38	71.60	72.52	65.29	62.79	63.85	60.68
InstAlign(Ours)	Swin-B	68.94	74.34	79.72	73.22	74.51	75.65	63.88	65.74	70.72

Table 1. Quantitative comparison of LLM-based, RES, and GRES methods across val, testA, and testB sets of gRefCOCO dataset. [†] denotes using external datasets.

4. Experiments

4.1. Experimental Setup

Datasets and Evaluation Metrics. Our experiments are conducted on two primary benchmarks in GRES: gRefCOCO [17] and Ref-ZOM [7], which derive images from COCO dataset [16, 26, 41]. We assess InstAlign using standard metrics on the gRefCOCO [17] and Ref-ZOM [7] datasets. For gRefCOCO, we employ cIoU, gIoU, and N-acc metrics, while for Ref-ZOM, we use mIoU, oIoU, and Acc metrics. Detailed descriptions of these datasets and metrics are provided in the supplementary material.

Implementation Details. Our model is implemented in PyTorch. Our model uses Swin-Transformer-B [22] as the visual encoder and we adopt RoBERTa [21] as our text encoder. The visual encoder is initialized with classification weights pre-trained on ImageNet22K [28]. We use $K = 9$ blocks of Phrase-Object Transformer in total.

We resize the image input to the resolution of 480×480 for both training and evaluation. We use the AdamW [23] optimizer with a batch size of 32. The learning rate is set to 10^{-4} and linear decreasing to 10^{-6} in 20 epochs. The entire training process takes approximately 24 hours on four NVIDIA A5000 GPUs.

4.2. Main Results

We evaluate InstAlign on the gRefCOCO [17] and Ref-ZOM [7] datasets, comparing our performance with state-of-the-art methods in both LLM-based, RES and GRES approaches. Tables 1 and 2 summarize the results, demon-

strating that InstAlign (highlighted in lavender) consistently outperforms existing approaches across all metrics and datasets.

On the gRefCOCO dataset (Table 1), InstAlign achieves a notable improvement in all metrics across all validation and test splits. Specifically, in the validation set, InstAlign attains the highest scores, with 68.94% in cIoU, 74.34% in gIoU, and 79.72% in N-acc. These scores exceed previous best-performing GRES models, such as LQMFormer [29], and significantly outperform RES and LLM-based methods, including LISA-7B [13] and GSVA-7B [37]. For the Ref-ZOM dataset (Table 2), InstAlign also achieves state-of-the-art results, with cIoU, gIoU, and N-acc surpassing all previous methods. In particular, InstAlign records a cIoU of 70.8%, gIoU of 71.1%, and an N-acc of 94.23%, demonstrating substantial improvements over both GRES methods like DMMI [7] and RES models such as LAVT [40]. These results confirm that InstAlign not only advances the current state of GRES but also sets new benchmarks for segmentation quality across diverse datasets, solidifying its robustness and adaptability in vision-language tasks.

4.3. Ablation Studies

We perform several ablation studies to evaluate the effectiveness of the key components in our InstAlign model on gRefCOCO [17] dataset. The results are listed in the Table 3. We highlight our default configuration with lavender.

Instance Supervision. We examine the effect of different instance supervision methods in Table 3(a). Without instance supervision, the model is trained only with the merged mask loss, achieving only 63.33% cIoU, 66.95%

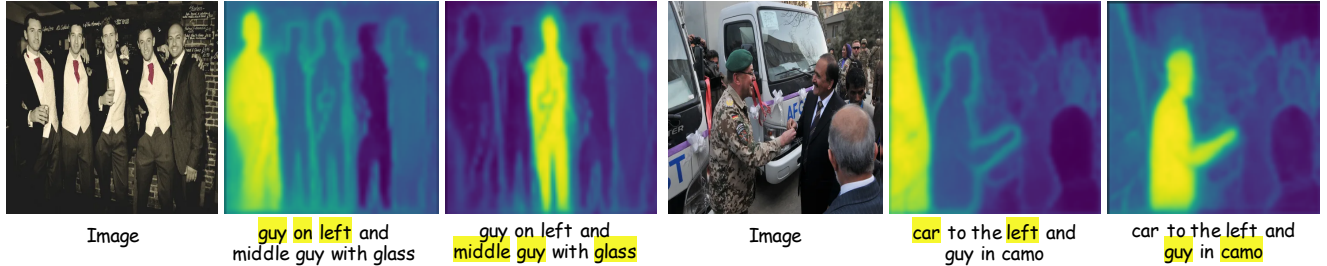


Figure 6. We visualize the segmentation heatmaps of top score queries and the corresponding alignment with the expression. We highlight words that are most aligned with each query. It can be seen that highlighted words can describe the instance it targets.

Method	Backbone	test		
		mIoU	oIoU	Acc
<i>LLM-based Methods</i>				
LISA-7B [†] [13]	SAM-ViT-H	65.39	66.41	93.39
GSVA-7B [†] [37]	SAM-ViT-H	68.13	68.29	94.59
<i>RES Methods</i>				
MCN [24]	ResNet-101	54.70	55.03	75.81
CMPC [20]	DarkNet-53	55.72	56.19	77.01
VLT [6]	ResNet-101	60.43	60.21	79.16
LAVT [40]	Swin-B	64.78	64.45	83.11
<i>GRES Methods</i>				
DMMI [7]	Swin-B	68.21	68.77	87.02
HDC [25]	Swin-B	69.31	68.81	93.34
InstAlign(Ours)	Swin-B	70.81	71.13	94.23

Table 2. Quantitative comparison of LLM-based, RES, and GRES methods on Ref-ZOM dataset. [†] denotes using external datasets.

gIoU, and 70.56% N-acc. Standard instance supervision without phrase alignment improves cIoU to 66.26%. However, our proposed Phrase-Aligned Instance Supervision further boosts performance to 68.94% cIoU, 74.34% gIoU, and 79.72% N-acc, demonstrating that incorporating Phrase-Object Alignment during instance matching improves segmentation accuracy.

Design options of Instance Aggregation. In Table 3(b), we explore various designs for the aggregation module, including fixed threshold instance selection and our AIA module with and without the PReLU activation. Among these, the AIA with PReLU setting achieves the highest performance. This indicates that adaptive weighting and PReLU activation effectively enhance the merging process.

No-target Predictor. The configuration of the no-target predictor also plays a critical role in segmentation accuracy. We compare four configurations in Table 3(c): using both Q_{global} and sentence features T_{sen} , only Q_{global} , T_{sen} alone, and averaging the object queries. The concatenation of global token Q_{global} and T_{sen} outperforms all others, achieving top scores in cIoU, gIoU, and N-acc. This setup captures both the global textual context and instance relevance to handle no-target scenarios effectively.

Setting	cIoU	gIoU	N-acc
<i>(a) Instance Supervision</i>			
None	63.33	66.95	70.56
Vanilla	66.26	70.32	76.19
Phrase-Aligned	68.94	74.34	79.72
<i>(b) Design option of aggregation module</i>			
Fixed selection	66.67	69.25	72.96
AIA w.o PReLU	68.13	72.35	78.22
AIA	68.94	74.34	79.72
<i>(c) No-target Predictor</i>			
Concat(Q_{global}, T_{sen})	68.94	74.34	79.72
Q_{global}	67.85	71.19	70.33
T_{sen}	64.29	67.91	75.55
Average all object queries	64.01	66.29	69.23
<i>(d) Number of queries</i>			
$N = 20$	67.64	72.67	77.25
$N = 50$	68.56	74.23	79.85
$N = 100$	68.94	74.34	79.72
$N = 200$	68.01	73.24	78.12
<i>(e) Transformer Decoder</i>			
Mask2Former [4]	44.43	47.42	55.58
ReLA [17]	67.16	69.23	74.56
POT	68.94	74.34	79.72

Table 3. Ablation study on the validation set of gRefCOCO.

Number of queries. We investigate the impact of the number of queries in Table 3(d), testing values of $N \in \{20, 50, 100, 200\}$. Our results show that $N = 100$ provides the best balance, achieving the highest cIoU, gIoU, and N-acc scores. Increasing the number of queries beyond 100 does not yield further improvement, while fewer queries lead to a drop in performance, suggesting that 100 queries provide optimal candidate instance coverage.

Transformer Decoder. Finally, we compare our POT with other decoders [4, 17] in Table 3(e). By utilizing the Mask2Former transformer decoder directly without any text information guidance, the model seems to randomly predict instances in the image, achieving 44.43% in cIoU. Incorporating ReLA [17] Decoder enhances the object queries with text features and with the support of the remaining of our

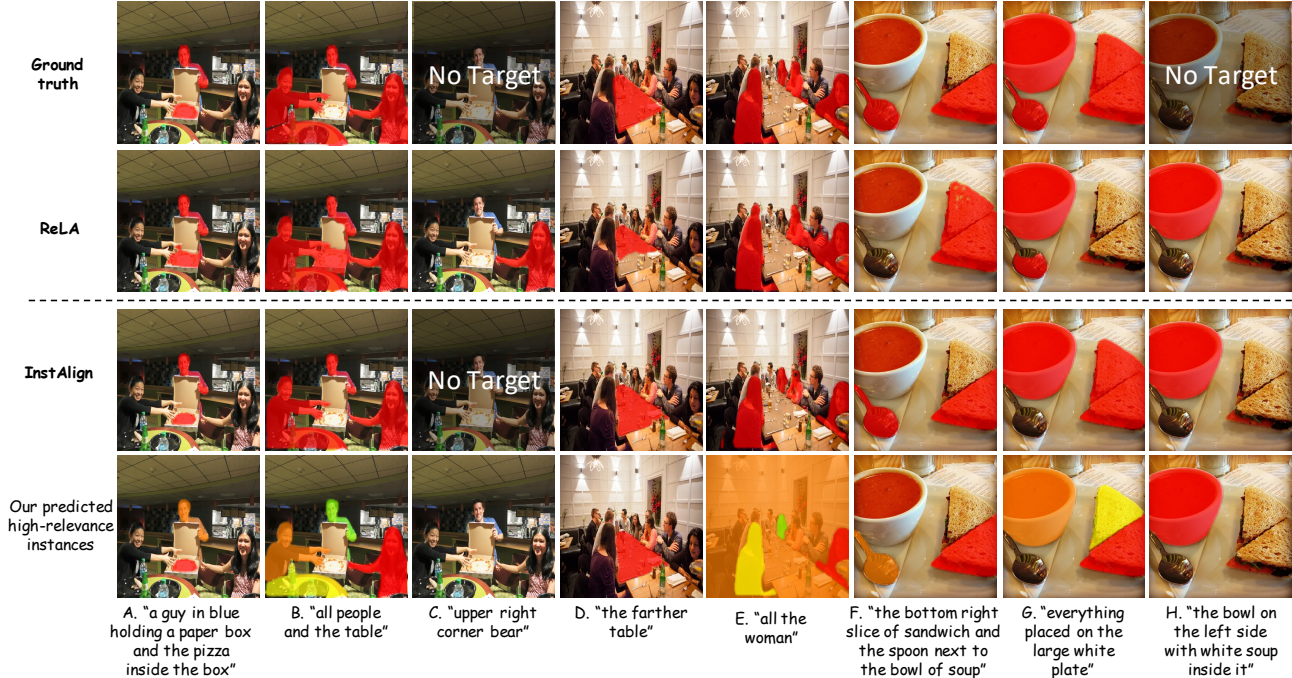


Figure 7. Visualization on gRefCOCO dataset. We compare our results with ReLA, which is the previous state-of-the-art method. We also show our high-relevance predicted instances in the last row. Best viewed in color.

architecture, improving the result to 67.17% in cIoU. Our POT decoder achieves the best result. This highlights the effectiveness of our transformer design in capturing cross-modal interactions to enhance both object queries and text features so that they can better align with each other.

4.4. Visualization

To demonstrate the effectiveness of InstAlign in handling complex referring expressions, we present qualitative visualizations comparing our method with the previous state-of-the-art model, ReLA, in Figure 7. In the last row, we show the high-scoring relevant instances predicted by InstAlign.

ReLA, lacking object-level reasoning, frequently over-segments (columns A, B, C, H), under-segments (columns D, G), or exhibits both issues (columns E, F). In contrast, InstAlign explicitly identifies relevant instances and effectively combines them into an accurate segmentation map. In column E, for the expression "all the women," InstAlign correctly segments three individual women at the instance level but includes an extra whole-image prediction, likely influenced by the word "all" in a specific query. However, our AIA effectively down-weights this broad instance, integrating relevant lower-scoring predictions to produce a refined segmentation for complex expressions.

5. Limitations and Future work

Our method is not without limitations. Despite its strong performance, InstAlign faces challenges in interpreting hierarchical or compositional relationships between objects and their attributes, particularly in no-target scenarios. Con-

sequently, the model may fail when expressions include attributes partially describing the target object while introducing conflicting information. For example, in the last column of Figure 7, InstAlign correctly segments "the bowl on the left side" but is distracted by the additional attribute "with the white soup inside it," resulting in inaccurate segmentation. These limitations highlight the need for improved contextual understanding and better handling of relationship dependencies to enhance performance in both complex expressions and no-target situations.

6. Conclusion

In this work, we presented InstAlign, a novel instance-aware model for Generalized Referring Expression Segmentation (GRES) to effectively address complex multi-object scenarios. By adapting instance segmentation frameworks and introducing a Phrase-Object Alignment, InstAlign explicitly identifies and associates individual object instances with specific textual phrases. Additionally, our Adaptive Instance Aggregation module enhances the integration of relevant instances, ensuring robust performance in complex multi-object and no-target scenarios. Extensive evaluations on the gRefCOCO and Ref-ZOM benchmarks showed that InstAlign outperforms state-of-the-art GRES and LLM-based methods, setting a new standard in the field. These advances pave the way for more precise and versatile multimodal applications in computer vision such as human-robot interaction and image editing.

References

- [1] Nicolas Carion, Francisco Massa, Gabriel Synnaeve, Nicolas Usunier, Alexander Kirillov, and Sergey Zagoruyko. End-to-End Object Detection with Transformers, 2020. arXiv:2005.12872. 2
- [2] Yi-Chia Chen, Wei-Hua Li, Cheng Sun, Yu-Chiang Frank Wang, and Chu-Song Chen. SAM4MLLM: Enhance Multi-Modal Large Language Model for Referring Expression Segmentation, 2024. arXiv:2409.10542. 2, 6
- [3] Bowen Cheng, Alex Schwing, and Alexander Kirillov. Per-Pixel Classification is Not All You Need for Semantic Segmentation. In *Advances in Neural Information Processing Systems*, pages 17864–17875. Curran Associates, Inc., 2021. 1, 3, 4
- [4] Bowen Cheng, Ishan Misra, Alexander G. Schwing, Alexander Kirillov, and Rohit Girdhar. Masked-attention Mask Transformer for Universal Image Segmentation. In *2022 IEEE/CVF Conference on Computer Vision and Pattern Recognition (CVPR)*, pages 1280–1289, New Orleans, LA, USA, 2022. IEEE. 1, 2, 3, 4, 7, 11
- [5] Yong Xien Chng, Henry Zheng, Yizeng Han, Xuchong Qiu, and Gao Huang. Mask Grounding for Referring Image Segmentation. In *2024 IEEE/CVF Conference on Computer Vision and Pattern Recognition (CVPR)*, pages 26563–26573, Seattle, WA, USA, 2024. IEEE. 2, 3, 12
- [6] Henghui Ding, Chang Liu, Suchen Wang, and Xudong Jiang. Vision-Language Transformer and Query Generation for Referring Segmentation. In *2021 IEEE/CVF International Conference on Computer Vision (ICCV)*, pages 16301–16310, Montreal, QC, Canada, 2021. IEEE. 1, 2, 6, 7, 11, 12
- [7] Yutao Hu, Qixiong Wang, Wenqi Shao, Enze Xie, Zhen-guo Li, Jungong Han, and Ping Luo. Beyond One-to-One: Rethinking the Referring Image Segmentation. In *2023 IEEE/CVF International Conference on Computer Vision (ICCV)*, pages 4044–4054, Paris, France, 2023. IEEE. 1, 2, 3, 5, 6, 7, 11, 12
- [8] Shaofei Huang, Tianrui Hui, Si Liu, Guanbin Li, Yunchao Wei, Jizhong Han, Luoqi Liu, and Bo Li. Referring Image Segmentation via Cross-Modal Progressive Comprehension. In *2020 IEEE/CVF Conference on Computer Vision and Pattern Recognition (CVPR)*, pages 10485–10494, Seattle, WA, USA, 2020. IEEE. 1
- [9] Ziling Huang and Shin’ichi Satoh. Referring Image Segmentation via Joint Mask Contextual Embedding Learning and Progressive Alignment Network. In *Proceedings of the 2023 Conference on Empirical Methods in Natural Language Processing*, pages 7753–7762, Singapore, 2023. Association for Computational Linguistics. 2
- [10] Sahar Kazemzadeh, Vicente Ordonez, Mark Matten, and Tamara Berg. ReferItGame: Referring to Objects in Photographs of Natural Scenes. In *Proceedings of the 2014 Conference on Empirical Methods in Natural Language Processing (EMNLP)*, pages 787–798, Doha, Qatar, 2014. Association for Computational Linguistics. 12
- [11] Namyup Kim, Dongwon Kim, Suha Kwak, Cuiling Lan, and Wenjun Zeng. ReSTR: Convolution-free Referring Image Segmentation Using Transformers. In *2022 IEEE/CVF Conference on Computer Vision and Pattern Recognition (CVPR)*, pages 18124–18133, New Orleans, LA, USA, 2022. IEEE. 2, 12
- [12] H. W. Kuhn. The Hungarian method for the assignment problem. *Naval Research Logistics Quarterly*, 2(1-2):83–97, 1955. eprint: <https://onlinelibrary.wiley.com/doi/pdf/10.1002/nav.3800020109>. 2, 4
- [13] Xin Lai, Zhuotao Tian, Yukang Chen, Yanwei Li, Yuhui Yuan, Shu Liu, and Jiaya Jia. LISA: Reasoning Segmentation via Large Language Model. In *2024 IEEE/CVF Conference on Computer Vision and Pattern Recognition (CVPR)*, pages 9579–9589, Seattle, WA, USA, 2024. IEEE. 2, 6, 7, 12
- [14] Feng Li, Hao Zhang, Huaizhe xu, Shilong Liu, Lei Zhang, Lionel M. Ni, and Heung-Yeung Shum. Mask DINO: Towards A Unified Transformer-based Framework for Object Detection and Segmentation, 2022. arXiv:2206.02777. 1
- [15] Weize Li, Zhicheng Zhao, Haochen Bai, and Fei Su. Bring Adaptive Binding Prototypes to Generalized Referring Expression Segmentation, 2024. arXiv:2405.15169 version: 1. 6
- [16] Tsung-Yi Lin, Michael Maire, Serge Belongie, James Hays, Pietro Perona, Deva Ramanan, Piotr Dollár, and C. Lawrence Zitnick. Microsoft COCO: Common Objects in Context. In *Computer Vision – ECCV 2014*, pages 740–755, Cham, 2014. Springer International Publishing. 6
- [17] Chang Liu, Henghui Ding, and Xudong Jiang. GRES: Generalized Referring Expression Segmentation. In *2023 IEEE/CVF Conference on Computer Vision and Pattern Recognition (CVPR)*, pages 23592–23601, Vancouver, BC, Canada, 2023. IEEE. 1, 2, 5, 6, 7, 11, 12
- [18] Fang Liu, Yuhao Liu, Yuqiu Kong, Ke Xu, Lihe Zhang, Bao-cai Yin, Gerhard Hancke, and Rynson Lau. Referring Image Segmentation Using Text Supervision. 2
- [19] Jiang Liu, Hui Ding, Zhaowei Cai, Yuting Zhang, Ravi Kumar Satzoda, Vijay Mahadevan, and R. Manmatha. PolyFormer: Referring Image Segmentation as Sequential Polygon Generation. In *2023 IEEE/CVF Conference on Computer Vision and Pattern Recognition (CVPR)*, pages 18653–18663, Vancouver, BC, Canada, 2023. IEEE. 2, 12
- [20] Si Liu, Tianrui Hui, Shaofei Huang, Yunchao Wei, Bo Li, and Guanbin Li. Cross-Modal Progressive Comprehension for Referring Segmentation. *IEEE Transactions on Pattern Analysis and Machine Intelligence*, 44(9):4761–4775, 2022. Conference Name: IEEE Transactions on Pattern Analysis and Machine Intelligence. 7, 11
- [21] Yinhan Liu, Myle Ott, Naman Goyal, Jingfei Du, Mandar Joshi, Danqi Chen, Omer Levy, Mike Lewis, Luke Zettlemoyer, and Veselin Stoyanov. RoBERTa: A Robustly Optimized BERT Pretraining Approach, 2019. arXiv:1907.11692. 3, 6, 11
- [22] Ze Liu, Yutong Lin, Yue Cao, Han Hu, Yixuan Wei, Zheng Zhang, Stephen Lin, and Baining Guo. Swin Transformer: Hierarchical Vision Transformer using Shifted Windows. In *2021 IEEE/CVF International Conference on Computer Vision (ICCV)*, pages 9992–10002, Montreal, QC, Canada, 2021. IEEE. 6
- [23] Ilya Loshchilov and Frank Hutter. Decoupled Weight Decay Regularization. 2018. 6, 11

- [24] Gen Luo, Yiyi Zhou, Xiaoshuai Sun, Liujuan Cao, Chenglin Wu, Cheng Deng, and Rongrong Ji. Multi-Task Collaborative Network for Joint Referring Expression Comprehension and Segmentation. In *2020 IEEE/CVF Conference on Computer Vision and Pattern Recognition (CVPR)*, pages 10031–10040, Seattle, WA, USA, 2020. IEEE. 7, 11
- [25] Zhuoyan Luo, Yinghao Wu, Yong Liu, Yicheng Xiao, Xiaoping Zhang, and Yujiu Yang. HDC: Hierarchical Semantic Decoding with Counting Assistance for Generalized Referring Expression Segmentation, 2024. arXiv:2405.15658. 1, 5, 6, 7
- [26] Junhua Mao, Jonathan Huang, Alexander Toshev, Oana Camburu, Alan Yuille, and Kevin Murphy. Generation and Comprehension of Unambiguous Object Descriptions. In *2016 IEEE Conference on Computer Vision and Pattern Recognition (CVPR)*, pages 11–20, Las Vegas, NV, USA, 2016. IEEE. 1, 6, 12
- [27] Hai Nguyen-Truong, E.-Ro Nguyen, Tuan-Anh Vu, Minh-Triet Tran, Binh-Son Hua, and Sai-Kit Yeung. Vision-Aware Text Features in Referring Image Segmentation: From Object Understanding to Context Understanding, 2024. arXiv:2404.08590. 2, 3
- [28] Olga Russakovsky, Jia Deng, Hao Su, Jonathan Krause, Sanjeev Sathesh, Sean Ma, Zhiheng Huang, Andrej Karpathy, Aditya Khosla, Michael Bernstein, Alexander C. Berg, and Li Fei-Fei. ImageNet Large Scale Visual Recognition Challenge. *International Journal of Computer Vision*, 115(3): 211–252, 2015. 6
- [29] Nisarg A. Shah, Vibashan VS, and Vishal M. Patel. LQMFormer: Language-Aware Query Mask Transformer for Referring Image Segmentation. In *2024 IEEE/CVF Conference on Computer Vision and Pattern Recognition (CVPR)*, pages 12903–12913, 2024. ISSN: 2575-7075. 1, 2, 5, 6, 12
- [30] Chao Shang, Zichen Song, Heqian Qiu, Lanxiao Wang, Fanman Meng, and Hongliang Li. Prompt-Driven Referring Image Segmentation with Instance Contrasting. In *2024 IEEE/CVF Conference on Computer Vision and Pattern Recognition (CVPR)*, pages 4124–4134, Seattle, WA, USA, 2024. IEEE. 2, 12
- [31] Wei Su, Peihan Miao, Huanzhang Dou, Gaoang Wang, Liang Qiao, Zheyang Li, and Xi Li. Language Adaptive Weight Generation for Multi-Task Visual Grounding. In *2023 IEEE/CVF Conference on Computer Vision and Pattern Recognition (CVPR)*, pages 10857–10866, Vancouver, BC, Canada, 2023. IEEE. 2
- [32] Carole H. Sudre, Wenqi Li, Tom Vercauteren, Sébastien Ourselin, and M. Jorge Cardoso. Generalised Dice overlap as a deep learning loss function for highly unbalanced segmentations, 2017. arXiv:1707.03237. 4, 5
- [33] Jiajin Tang, Ge Zheng, Cheng Shi, and Sibe Yang. Contrastive Grouping with Transformer for Referring Image Segmentation. In *2023 IEEE/CVF Conference on Computer Vision and Pattern Recognition (CVPR)*, pages 23570–23580, Vancouver, BC, Canada, 2023. IEEE. 2, 12
- [34] Zhaoqing Wang, Yu Lu, Qiang Li, Xunqiang Tao, Yandong Guo, Mingming Gong, and Tongliang Liu. CRIS: CLIP-Driven Referring Image Segmentation. In *2022 IEEE/CVF Conference on Computer Vision and Pattern Recognition (CVPR)*, pages 11676–11685, New Orleans, LA, USA, 2022. IEEE. 1, 2, 5, 6, 12
- [35] Jiannan Wu, Yi Jiang, Peize Sun, Zehuan Yuan, and Ping Luo. Language as Queries for Referring Video Object Segmentation. In *2022 IEEE/CVF Conference on Computer Vision and Pattern Recognition (CVPR)*, pages 4964–4974, New Orleans, LA, USA, 2022. IEEE. 2
- [36] Jianzong Wu, Xiangtai Li, Xia Li, Henghui Ding, Yunhai Tong, and Dacheng Tao. Towards Robust Referring Image Segmentation, 2023. arXiv:2209.09554. 2
- [37] Zhuofan Xia, Dongchen Han, Yizeng Han, Xuran Pan, Shiji Song, and Gao Huang. GSVA: Generalized Segmentation via Multimodal Large Language Models. In *2024 IEEE/CVF Conference on Computer Vision and Pattern Recognition (CVPR)*, pages 3858–3869, Seattle, WA, USA, 2024. IEEE. 2, 6, 7, 12
- [38] Zunnan Xu, Zhihong Chen, Yong Zhang, Yibing Song, Xiang Wan, and Guanbin Li. Bridging Vision and Language Encoders: Parameter-Efficient Tuning for Referring Image Segmentation. In *2023 IEEE/CVF International Conference on Computer Vision (ICCV)*, pages 17457–17466, Paris, France, 2023. IEEE. 2, 3
- [39] Yuhuan Yang, Chaofan Ma, Jiangchao Yao, Zhun Zhong, Ya Zhang, and Yanfeng Wang. ReMamber: Referring Image Segmentation with Mamba Twister, 2024. arXiv:2403.17839. 2
- [40] Zhao Yang, Jiaqi Wang, Yansong Tang, Kai Chen, Hengshuang Zhao, and Philip H.S. Torr. LAVT: Language-Aware Vision Transformer for Referring Image Segmentation. In *2022 IEEE/CVF Conference on Computer Vision and Pattern Recognition (CVPR)*, pages 18134–18144, New Orleans, LA, USA, 2022. IEEE. 2, 5, 6, 7, 11, 12
- [41] Licheng Yu, Patrick Poirson, Shan Yang, Alexander C. Berg, and Tamara L. Berg. Modeling Context in Referring Expressions. In *Computer Vision – ECCV 2016*, pages 69–85, Cham, 2016. Springer International Publishing. 6
- [42] Licheng Yu, Zhe Lin, Xiaohui Shen, Jimei Yang, Xin Lu, Mohit Bansal, and Tamara L. Berg. MAttNet: Modular Attention Network for Referring Expression Comprehension. In *2018 IEEE/CVF Conference on Computer Vision and Pattern Recognition*, pages 1307–1315, Salt Lake City, UT, 2018. IEEE. 5, 6
- [43] Xizhou Zhu, Weijie Su, Lewei Lu, Bin Li, Xiaogang Wang, and Jifeng Dai. Deformable DETR: Deformable Transformers for End-to-End Object Detection, 2021. arXiv:2010.04159. 3

Instance-Aware Generalized Referring Expression Segmentation

Supplementary Material

In this Supplementary, we first provide more details about the datasets and metrics we use in this work. We then provide more about our implementation details. Finally, we show more analysis of our experiments in both GRES and traditional RES tasks.

7. Details about Datasets and Metrics

7.1. gRefCOCO

Proposed by Liu *et al.* [17], the gRefCOCO dataset consists of 19,994 images of 60,287 distinct instances described by 278,232 language expressions. These annotations include 80,022 multi-target and 32,202 no-target samples.

For evaluation on gRefCOCO dataset, we use the following metrics:

- **cIoU** (cumulative Intersection over Union): Measures the total pixel intersection over the total pixel union across the validation split, offering a holistic view of segmentation performance.
- **gIoU** (generalized Intersection over Union): Averages the per-image IoU across all samples to evaluate segmentation precision at the image level. For no-target samples, the per-image IoU is 1 if we predict correctly a no-target sample and 0 in the other cases.
- **N-acc** (no-target accuracy): Quantifies the accuracy of no-target identification, i.e., how well the model identifies cases where no target is present.

7.2. Ref-ZOM

Proposed by Huet *et al.* [7], the Ref-ZOM is similar to gRefCOCO, introducing the one-to-one, one-to-many, and one-to-zero referring expressions. These cases correspond to the single-target, multi-target, and no-target samples in gRefCOCO, respectively. Ref-ZOM dataset consists of 55,078 images of 74,942 annotated instances, which includes 41,842 annotated objects under one-to-many settings, 11,937 one-to-zero samples, and 42,421 one-to-one objects.

For Ref-ZOM, gIoU and cIoU are substituted to the equivalent metrics in RES, mIoU and oIoU. However, different from gRefCOCO, mIoU and gIoU only count for one-to-one and one-to-many samples. For one-to-zero samples, we use the accuracy (acc) metric, which measures the classification performance on empty-target expressions.

7.3. Instances ground truth

While the metrics to measure the performance for GRES task are based on the binary ground-truth mask, both gRefCOCO [17] and Ref-ZOM [7] datasets provide instance mask annotations for each expression. We utilize these annotations for our instance supervision.

8. Implementation Details

Our model is optimized using AdamW [23] optimizer with the initial learning rate of 10^{-4} and linear decreasing to 10^{-6} after 20 epochs. For instance matching, the coefficients are set as $\lambda_{score} = 2$, $\lambda_{mask} = 5$, $\lambda_{phrase} = 1$. In the loss function, we set $\lambda_{merged} = 5$, $\lambda_{inst} = 1$, and $\lambda_{nt} = 0.1$. RoBERTa-base [21] is used as the Text Encoder to extract language features and the Pixel Decoder comprises 6 layers of Deformable Transformer, following Mask2Former [4].

Method	One-to-One		One-to-Many		Overall Targets		One-to-Zero
	oIoU	mIoU	oIoU	mIoU	oIoU	mIoU	Acc
MCN [24]	52.09	53.14	58.04	57.21	55.05	54.70	75.81
CMPC [20]	52.46	52.89	60.23	60.27	56.19	55.72	77.01
VLT [6]	59.07	58.96	61.42	62.79	60.21	60.43	79.26
LAVT [40]	63.21	64.56	65.69	65.14	64.45	64.78	83.11
DMMI [7]	65.43	66.83	72.20	70.44	68.77	68.21	87.02
InstAlign(Ours)	66.36	68.41	76.77	75.09	71.13	70.81	94.23

Table 4. Quantitative comparison across 3 cases of Ref-ZOM dataset.

9. More quantitative results

9.1. Ref-ZOM

Table 1 showcases the results of our method compared to state-of-the-art methods across one-to-one, one-to-many, and one-to-zero cases in the Ref-ZOM dataset. Our model demonstrates significant improvements across all scenarios. In one-to-one cases, InstAlign surpasses prior SOTA with a margin of 0.93% and 2.58% in terms of oIoU and mIoU, respectively, showcasing our precision in identifying individual objects. In one-to-many cases, our model outperforms DMMI [7] with a large margin of 4.47% and 4.65% in oIoU and mIoU. For the no-target scenario, the Acc score of 94.23% indicates our model’s ability to accurately determine when no valid target is present compared to previous approaches.

These results highlight the effectiveness of explicitly predicting relevant instances and adaptive instance aggregation, enabling accurate segmentation for complex expressions.

Method	Backbone	RefCOCO			RefCOCO+			RefCOCOg	
		val	test A	test B	val	test A	test B	val	test
VLT [6]	Darknet-53	65.65	68.29	62.73	55.50	59.20	49.36	52.99	56.65
ReSTR [11]	ViT-B/16	67.22	69.30	64.45	55.78	60.44	48.27	-	-
CRIS [34]	ResNet-101	70.47	73.18	66.10	62.27	68.08	53.68	59.87	60.36
LAVT [40]	Swin-B	72.73	75.82	68.79	62.14	68.38	55.10	61.24	62.09
ReLA [17]	Swin-B	73.82	76.48	70.18	66.04	71.02	57.65	65.00	65.97
DMMI [7]	Swin-B	74.14	77.13	70.16	63.98	69.73	57.03	61.98	63.46
LQMFormer [29]	Swin-B	74.16	76.82	71.04	65.91	71.84	57.59	64.73	66.04
CGFormer [33]	Swin-B	74.75	77.30	70.64	64.54	71.00	57.14	62.51	64.68
PolyFormer [†] [19]	Swin-B	74.82	76.64	71.06	67.64	72.89	59.33	67.76	69.05
LISA-7B [†] [13]	SAM-ViT-H	74.1	76.5	71.1	62.4	67.4	56.5	66.4	68.5
GSVA-7B [†] [37]	SAM-ViT-H	77.2	78.9	73.5	65.9	69.6	59.8	72.7	73.3
Prompt-RIS [†] [30]	SAM-ViT-B/16	76.36	80.37	72.29	67.06	73.58	58.96	64.79	67.16
MagNet [‡] [5]	Swin-B	76.55	78.27	72.15	68.10	73.64	61.81	67.79	69.29
InstAlign(Ours)[‡]	Swin-B	78.05	80.02	75.03	68.32	72.85	60.15	73.47	75.73

Table 5. Comparison with SOTA methods in RES task using the oIoU metric. [‡] indicates combining the train splits from these 3 datasets with test images removed to prevent data leakage. [†] indicates using additional data beyond RefCOCO, RefCOCO+, and G-Ref.

9.2. Performance on Traditional RES

While our primary focus is addressing multi-target scenarios in Generalized Referring Expression Segmentation, we also evaluate our model on the traditional RES task to provide a broader performance perspective. We follow MagNet [5] to combine the train splits from 3 datasets RefCOCO, RefCOCO+ [10], and RefCOCOg [26] with test images removed to prevent data leakage. As shown in Table 2, while InstAlign is designed for GRES, it also performs competitively on traditional RES benchmarks. Notably, on the challenging RefCOCOg dataset, InstAlign surpasses the previous SOTA by significant margins of 5.68% and 6.44% in validation and test splits, respectively.

This indicates that our instance-aware reasoning and phrase-object alignment are beneficial even in traditional RES, suggesting broader applicability.